Available online at www.sciencedirect.com
SCIENCE DIRECT
Polymer 47 (2006) 1259–1266
polymer
www.elsevier.com/locate/polymer

Identification of charge carriers in the conduction mechanism of an alternated copolymer of poly(aniline) and poly(phenylene sulfide)

Fernanda Ferraz Camilo Bazito, Susana Inés Córdoba de Torresi *

Instituto de Química, Universidade de São Paulo, CP 26077, 05513-970 São Paulo-SP, Brazil

Received 12 August 2005; received in revised form 23 November 2005; accepted 25 November 2005
Available online 10 January 2006

Abstract

In this paper, we have investigated the electrochemical behavior of a soluble copolymer of poly(aniline) (PANI) and poly(phenylene sulfide) in organic media. By using 'in situ' UV–vis and Raman spectroscopies, it was proved that during the oxidation of the first cycle, polarons and bipolarons are formed consecutively, due to the loss of electrons from the nitrogen and sulfur, respectively. In addition, it was verified that the formation of polarons is reversible while the formation of bipolarons is irreversible. In the second and subsequent cycles, only one reversible redox process is observed. This process corresponds to the transformation of polarons to bipolarons and vice versa. The 'in situ' resistance measurements have indicated that bipolarons are the charge carriers for doped PPSA, distinctly than it was observed for PANI.

Keywords: Poly(aniline); Poly(phenylene sulfide); PPSA

1. Introduction

The main structural characteristics in conductive polymers are the linearity and rigidity of the molecule, that make these materials insoluble and infusible and, therefore, of difficult processability. Poly(aniline) (PANI) has been defined as a insoluble and infusible material under usual conditions. Therefore, several strategies to induce more solubility and processability have been investigated (substituted PANI, copolymers and blends) [1–5].

Poly(phenylene sulfide) (PPS) belongs to the same class of PANI, in the sense that both polymers have certain mobility in the main chain due to the addition of a heteroatom [6]. This polymer presents high crystallinity, good thermal stability and mechanical resistance. These favorable features allow its application in the industry as a high performance engineering plastic [7–9].

The preparation of a new copolymer containing phenylene sulfide (the monomer of PPS) and phenylene amine units (the monomer of PANI) distributed alternately could result in a material with lower crystallinity than its respective homopolymers and thereby more soluble and processable.

This new copolymer, denominate poly(phenylenesulfide phenyleamine) (PPSA) (Fig. 1), was synthesized for the first time in 1996 [10] and ever since it has been studied due to its interesting properties, such as mechanical stability and electrical conductivity. The polymer is an amorphous material with excellent thermal stability and good solubility in several organic solvents (THF, DMSO, DMF and NMP). In addition, when PPSA is chemically doped with $SbCl_5$ and $FeCl_3$, the resulting films show conductivity values of 0.2 and 1.4 S cm^{-1}, respectively [10,11].

Electrochemical studies carried out in organic media have shown that PPSA is oxidized in two stages and the insertion and expulsion of anions is the main process occurring during the electrochemical doping [11,12].

Due to its low oxidation potential, amorphous structure, high thermal stability and easy processability, PPSA have become a promising candidate for use in LEDs [13].

In this paper, we have investigated the electrochemical doping of PSSA in organic media, aiming to elucidate the redox mechanism and free carrier (polaron or bipolaron) occurring during the doping process by spectroscopic techniques coupled to cyclic voltammetry.

* Corresponding author. Tel.: +55 11 30912350; fax: +55 11 38155579.
E-mail address: storresi@iq.usp.br (S.I. Córdoba de Torresi).

0032-3861/$ - see front matter © 2005 Elsevier Ltd. All rights reserved.
doi:10.1016/j.polymer.2005.11.076

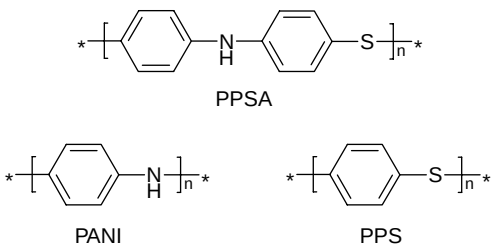

Fig. 1. Structure of poly(phenylenesulfide phenyleneamine) (PPSA).

2. Experimental part

2.1. Chemical and substrates

The copolymer PPSA was prepared following the procedure have already described in the literature [10,11].

Acetanilide (Aldrich, 97%) was recrystallized from a water/ethanol mixture. Thioanisole (Aldrich, 99%) was distilled under reduced pressure. Methanesulfonic acid (Aldrich, 99%) was heated with P_2O_5 at 100 °C for 30 min and distilled under reduced pressure before use. Pyridine (Aldrich, 99%) was refluxed with potassium hydroxide, followed by distillation at room pressure. Commercial bromine (Aldrich, 99%) was dried with sulfuric acid before the use.

All supporting electrolytes were dried at 80 °C under reduced pressure. The other chemicals were used as received. The solvents used in the reactions and electrochemical experiments were dried by conventional methods and freshly distilled under argon.

2.2. Electrodes

The surface of the Au and Pt electrodes were polished with Al_2O_3 powder and then washed with deionized water and acetone.

ITO substrates with resistivity of 20 Ω/sq from Delta Technologies Company were used. The ITO substrates were cleaned using acetone in an ultrasonic cleaner for 10 min before the use.

2.3. Dynamic light scattering

The light scattering measurements were performed using a Malvern 4700 MW equipment, equipped with a 25 mW He/Ne laser (Spectra-Physics Model 127), operating at 632.8 nm. The d*n*/d*c* values were determined in an Abbé-type refractomer (Bellingham and Stanley, model 60/ED), using a He/Ne laser (Spectra-Physics Model 127) as light source. The d*n*/d*c* obtained for the polymer in THF was 0.426 mL g^{-1}.

The polymeric solutions in THF were filtered by using millipore 0.22 μm membrane before the use.

The weight average molar mass (M_w) was determined by measuring the intensity of the scattered light in several angles and in different concentrations (2–10 g L^{-1}) and analyzing the data by Zimm methodology [14].

2.4. Raman spectroscopy

Raman spectra were recorded on a Renishaw Raman Imaging Microscope (System 3000), connected to a CCD detector (Wright, 600×400 pixels), using the 632.8 nm excitation radiation (He–Ne laser-spectra physics, model 127).

All baseline corrections were made manually and all spectra were normalized, using the solvent band as internal reference. In the experiments carry out in acetonitrile, it was utilized the band at 2253 cm^{-1} as reference, which corresponds to the C–N triple bond stretching. In propylene carbonate, the band at 2938 cm^{-1}, attributed to C–H aliphatic bond stretching was considered as internal standard.

Three aliquots of 2.0 μL of the polymeric solution of PPSA in THF (5.0 mg of polymer in 1.0 mL of solvent) were deposited on the Pt electrode by casting.

2.5. 'In situ' resistance

In situ resistance measurements were made using locally designed circuitry and a photolithographically prepared set of adjacent electrode pairs of gold (10 μm gap between two adjacent electrodes) [15].

For these measurements, the PPSA film was formed on a gold electrode by casting, using three aliquots (2.0 μL ea.) of a polymeric solution of PPSA in THF (5.0 mg mL^{-1}).

2.6. UV–vis spectroscopy

The UV–vis spectra were recorded in a HEWLETT PACKARD spectrophotometer model 8453, using quartz cell (1 cm path length). For the 'in situ' measurements the spectrophotometer was coupled to an EG&G potentiostat (model 362). A glass cuvette (1 cm path length) was utilized as spectroelectrochemical cell. The ITO electrode covered with a PPSA film was placed in the optical path of the spectrophotometer.

The spectra were registered from 350 to 900 nm. The PPSA film deposited on ITO was prepared by depositing five successive aliquots of 10 μL of the PPSA solution (5.0 mg of polymer in 1.0 mL de THF).

2.7. Cyclic voltammetry

Cyclic voltammetric measurements were performed with an Autolab/PGSTAT-30 (Eco Chemie) potentiostat/galvanostat connected to a microcomputer. The experiments were carried out in a single compartment electrochemical cell, using Pt as counter electrode. In all experiments a silver wire was used as quasi-reference electrode but all potentials are normalized to the ferrocene/ferrocinium (Fc/Fc^+) redox couple in the same electrolytic solution.

The polymeric film was deposited on the electrode (Au, Pt and ITO) by casting, using a PPSA solution (2.5 mg in 5.0 mL de THF). It was deposited three aliquots of 2.0 μL consecutively.

3. Results and discussion

3.1. Preparation and characterization

The PPSA was synthesized in five consecutive steps, following the procedure described in the literature (Scheme 1) [10,11,16].

PPSA was spectroscopically characterized by ^{1}H and ^{13}C NMR, FTIR and UV–vis spectroscopy. These spectroscopic data have shown that this material is structurally well-defined and only 1,4-linkages of the phenylene units are present. The copolymer presents good thermal stability with a glass transition temperature (T_g) of 145 °C and decomposition temperature above 360 °C (see Supporting Information). The absence of melting point is coherent with its amorphous character. The molar mass was estimated by static light scattering to be $M_w = 167{,}000$ g mol^{-1}. This value was also determined by size-exclusion chromatography in THF ($M_n = 109{,}000$ and $M_w = 260{,}000$) and membrane-osmometric measurements in DMF ($M_n = 110{,}000$) [11]. To date, this copolymer presents much higher molar mass than PANI. By gel permeation chromatography, the molar masses of PANI are reported to be $M_n = 80{,}000$ for electrochemically produced [17] and $M_n = 25{,}000$ for chemically synthesized PANI [18].

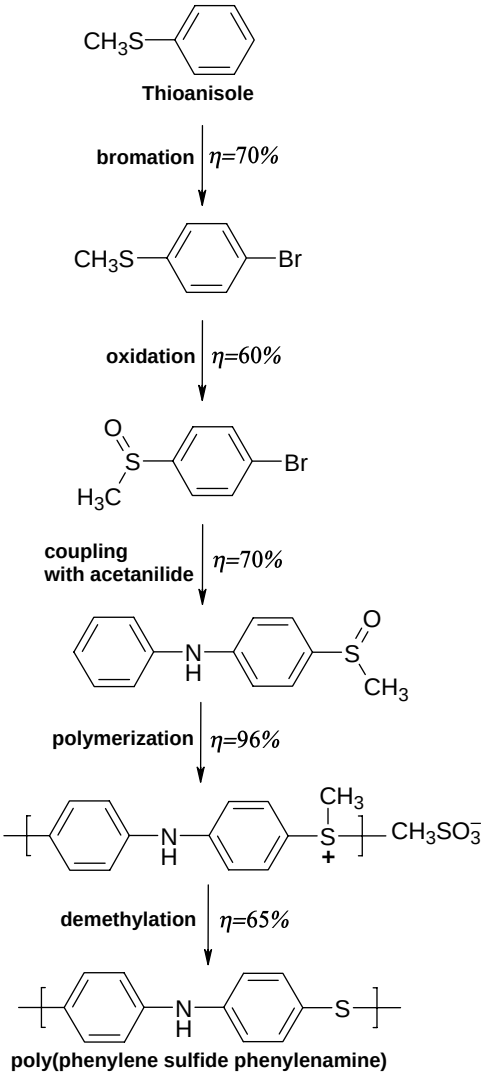

Scheme 1. Synthetic route for preparation of PPSA.

3.2. Espectroelectrochemical characterization

The cyclic voltammograms of a PPSA film deposited on a Pt electrode measured using two different scan rates in the potential window from −0.2 to 2.0 V are shown in Fig. 2.

In the first scan (Fig. 2(A)), only a wide anodic wave centered at 1.0 V and a cathodic wave at 0.2 V were observed. The charge associated with the reduction process is smaller than that obtained for the oxidation, indicating that the oxidation of PPSA is only partially reversible. In the subsquent scans, the redox processes become more reversible, considering the higher simetry between the cathodic and anodic peaks and the charges envolved in both processes. The current decreases gradually and after ten cycles the film losses its electroactivity. By using slower scan rate (Fig. 2(B)), the cyclic voltammogram is more defined and two anodic peaks were recorded during the first cycle, indicating that this redox process occur in two steps. In analogy to PANI, probably the oxidation of PPSA is accompained by insetion of anions to maintain the electroneutrality, instead of the expulsion of cations. In turn, when this polymer is reduced, these dopant anions leave the film. It is worthy to note that due to the partial reversibility observed during the first cycle, a large amount of perclorate ions remains inside the film. A complete investigation by electrochemical quartz crystal microbalance (EQCM) about the redox process of PPSA using diferent solvent/electrolyte mixtures were performed and these results

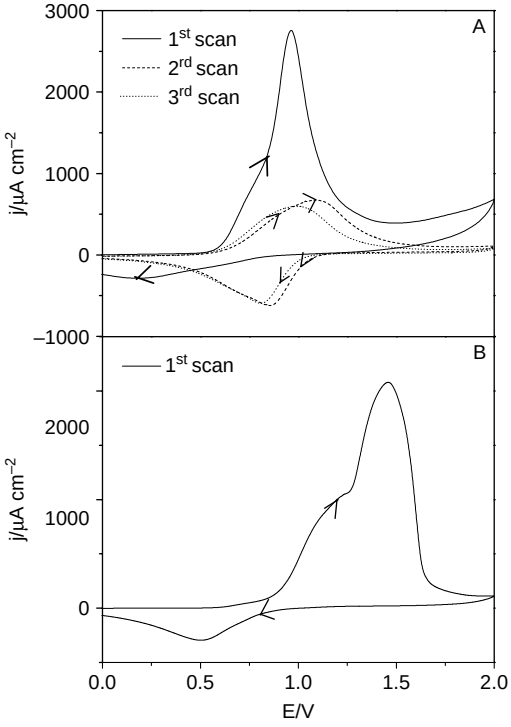

Fig. 2. Cyclic voltammograms of a PPSA film deposited on Pt electrode in 0.2 M $LiClO_4$/ACN (A) $v = 0.01$ V s^{-1} (B) $v = 0.001$ V s^{-1}.

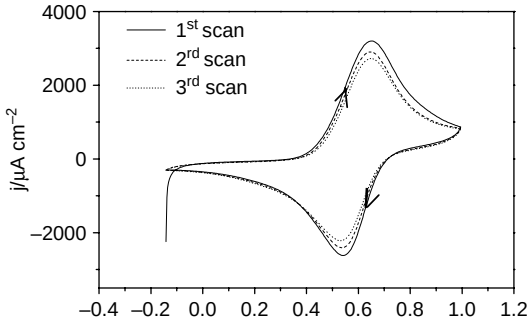

Fig. 3. Cyclic voltammogram of a PPSA film deposited on Pt electrode from −0.20 to 1.00 V (v=0.01 V s^{-1}).

agree with the above statement. The complete EQCM study will be discussed in another publication.

An additional cyclic voltammetry experiment of a PPSA film deposited on Pt, using a restricted potential range from −0.2 to 1.00 V (Fig. 3) has shown only one reversible redox process, similar to PANI [19–22]. This indicates that the presence of sulfur atom could be the main reason for the irreversibility of the PPSA during the electrochemical process and the nitrogen atom should be the first site to be oxidized in a reversible process.

3.3. In situ UV–vis spectroscopy

Fig. 4 shows the UV–vis spectra of a PPSA film recorded at selected potentials during the corresponding first cycle in 0.2 M $LiClO_4$/acetonitrile. The attributions of the bands in the spectra are based on previous papers about spectroeletrochemical studies of PANI [23,24] and other conductive polymers [25].

The first spectrum registered at −0.2 V (Fig. 4(a)) exhibits only one absorption peak below 350 nm. This band corresponds to the electronic transition between the conduction band (CB) and the valence band (VB) (Fig. 5(A)—transition 1). When the potential reaches 0.60 V, three new bands at 410,

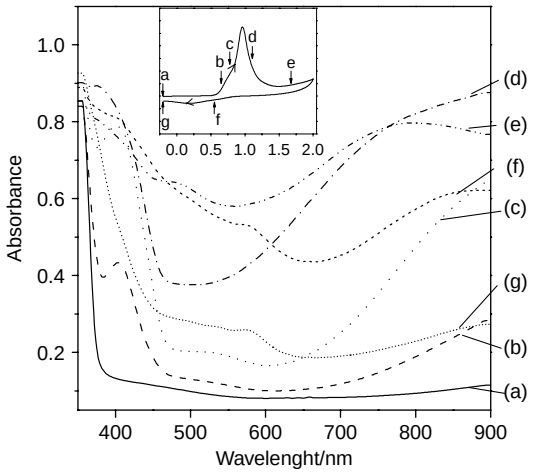

Fig. 4. Absorption spectra of PPSA film recorded during the first scan potential range: −0.2–2.0 V (v=0.01 V s^{-1}) (a) −0.20 V (b) 0.60 V (c) 0.80 V (d) 1.20 V (e) 1.60 V (f) 0.50 V (g) −0.20 V.

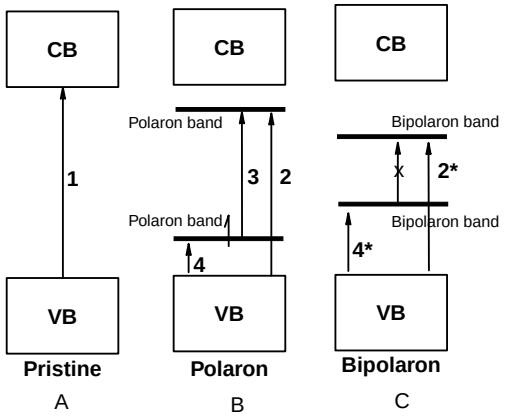

Fig. 5. Electronic transitions of different oxidized species of the PPSA based on the band model.

540 nm and higher than 900 nm emerge (Fig. 4(b)). The spectra collected from 0.60 to 1.20 V (Fig. 4(b)–(d)) present similar shapes, showing continuous increase in the intensity of these bands as the oxidation proceeds. These transitions are due to the appearance of intermediate electronic levels between the bandgap. These bands correspond to the electronic transitions shown in Fig. 5(B) noted as 2, 3 and 4. Further increase of the potential to 1.40 V leads to gradual shifts of the bands at 410 and 900 nm to lower and higher energies, respectively (Fig. 5(C)—transitions 4* and 2*). It was also observed the disappearance of the absorption at λ_{max}=540 nm. These changes are consistent with the appearance of two new levels more distant from the VB and CB than the respective polaronic bands (compare Fig. 5(B) and (C)). During the reduction, a general inverse behavior was observed. In the spectra collected from 0.60 to −0.20 V (Fig. 4(f) and (g)), the appearance of the band at 580 nm and the gradual shifts of the bands at 490 and 800–410 and 900 nm, indicates the modification of the intermediate levels. Finally, comparing the spectrum of pristine PPSA (Fig. 4(a)) with that obtained at the end of the first scan (Fig. 4(g)), we can confirm the presence of semi-oxidized species and thereby the partial reversibility of this cycle.

Fig. 6 shows the set of absorption spectra obtained during the second voltammetric scan. During the oxidation, the spectra recorded from −0.2 to 0.80 V (Fig. 6(a) and (b)) present three bands at 410, 580 nm and λ_{max}>900 nm, indicating that polarons are the species responsible for the electronic transitions. The spectra recorded after 1.00 V (Fig. 6(c)) acquire similar characteristics to that registered at 1.20 V during the oxidation of the first scan, where bipolarons are formed (Fig. 4(e)). During the reduction, the reappearance of the band at 580 nm (Fig. 5(B)—transition 3) and the shifts of the bands at 490 and 800–410 and >900 nm, respectively, suggest the formation of polarons. The reversibility of the second and subsequent cycles is in agreement with the similarity of the spectra registered in the beginning and at the end of each respective cycle (compare Fig. 6(a) and (e)).

An ‘in situ’ UV–vis experiment recorded in the potential range from −0.20 to 0.80 V was useful to investigate the

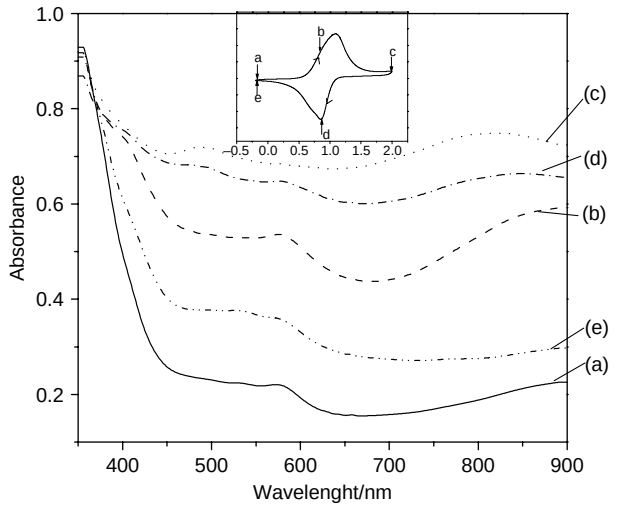

Fig. 6. Absorption spectra of a PPSA film registered during the second scan.

reversibility of the formation of polarons observed in the CV experiment recorded in the potential range from −0.20 to 1.00 V (Fig. 3). The coincidence between the spectra registered at the beginning and at the end of this cycle is in agreement with the reversibility shown in the cyclic voltammetry.

3.4. 'In situ' Raman spectroscopy

In order to investigate the structural modifications that occur during the electrochemical doping of the PPSA, we carried out 'in situ' Raman measurements of PPSA films deposited on Pt electrodes by using excitation line at 632.8 nm in 0.2 M $LiClO_4$/ACN. Fig. 8 shows the Raman spectra of a PPSA film recorded at different potentials during the first voltammetric scan.

In the pristine form (Fig. 7(a)), PPSA exhibits four bands. Those at 1088, 1230 and 1600 cm^{-1} are clearly assigned to the C–S, C–N and C–C aromatic bond stretching vibrations, respectively. In addition, the band at 1181 cm^{-1} is attributed to C–H in-plane bending of the aromatic rings.

The first changes observed during the oxidation of the PPSA occur at 0.50 V. In the spectra recorded at 0.50 V (Fig. 7(b)) and 0.60 V (Fig. 7(c)), it was noted the appearance of bands at 1314 and 1359 cm^{-1}, which are inherently associated to the presence of $C–N^{\cdot+}$ (distinct conformations). The decrease of the band at 1600 cm^{-1} together with the appearance of two others at 1536 and 1583 cm^{-1} indicates the presence of polarons. These bands were also observed at initial stages of PANI oxidation, where polarons are found predominantly [26–29]. These data agree with the appearance of a shoulder at 1152 cm^{-1} that is assigned to C–H in-plane bending deformation of the semi-quinoid units. It is worth to note that the band at 1088 cm^{-1} does not change, indicating that the sulfur atom has not been oxidized yet. Thereby, we conclude that in the first oxidation stage, the N atom is the only heteroatom to be oxidized.

When the potential reaches 0.70 V (Fig. 7(d)), several alterations are observed. Comparing with the spectrum

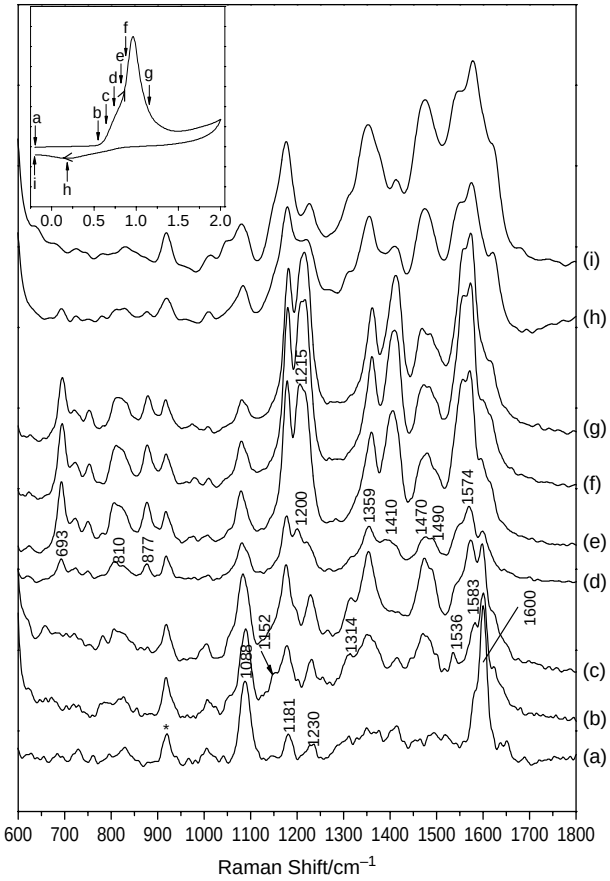

Fig. 7. Raman spectra of a PPSA film recorded at different potentials during the first scan-potential range: −0.2–2.0 V (a) −0.20 V (b) 0.50 V (c) 0.60 V (d) 0.70 V (e) 0.80 V (f) 0.90 V (g) 1.20 V (h) 0.20 V (i) −0.20 V.

collected at 0.60 V (Fig. 7(c)), it was noted the appearance of bands at 693, 810, 877 and 1410 cm^{-1}, which suggests the presence of quinoid species [30]. In addition, the concomitant decrease of the band at 1088 cm^{-1} is observed, since bipolarons (quinoids units) can be formed only after the oxidation of the sulfur heteroatom. Finally, the change of the C–S single bond character is corroborated by the appearance of the band at 1200 cm^{-1}, attributed to C=S stretching [31]. From 0.80 V onwards (Fig. 7(e)–(g)), the intensity of the bands corresponding to the bipolaronic structures increase markedly and the spectra become more defined. It is important to note that the bands at 1200 cm^{-1} (νC=S) and 1230 cm^{-1} (νC–N), observed at 0.70 V, become only one at 1215 cm^{-1}. The spectra registered after 0.80 V are very similar, independently on the potential applied, this fact being coherent with the resonant situation with the laser energy.

During the reduction, the main changes observed in the spectra recorded at 0.20 V (Fig. 7(h)) and −0.20 V (Fig. 7(i)), compared with that obtained at 1.20 V (Fig. 7(g)) are: the decrease of the bands at 1410, 877, 810 and 693 cm^{-1} that are related to the presence of quinoid units. The band at 1088 cm^{-1} remains unaltered during the reduction, indicating that, once oxidized, the sulfur site is not reduced again. The presence of bands assigned to oxidized units (semiquinoid

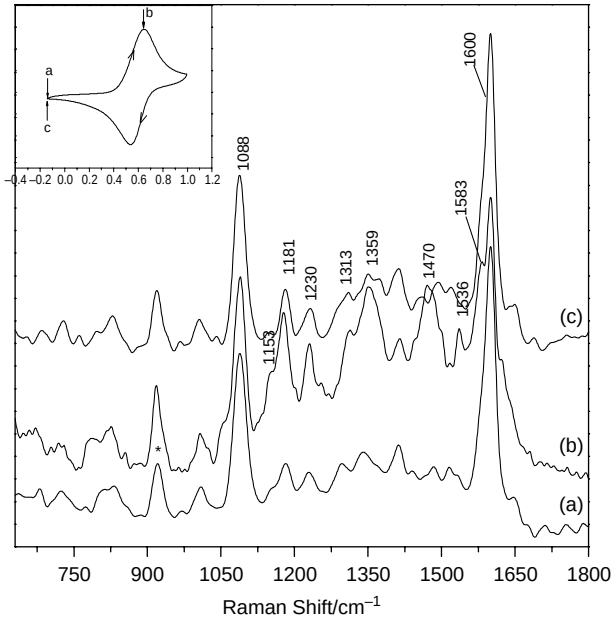

Fig. 8. Raman spectra of a PPSA film recorded at different potential during the first scan-potential range: −0.20–0.80 V (a) −0.20 V (b) 0.60 V (c) −0.20 V.

units) in the spectrum recorded at the end of this cycle (Fig. 7(i)) confirms the partial reversibility of the first cycle.

The reversible formation of polarons in the first stage of the oxidation of the PPSA shown by cyclic voltammetry (Fig. 3) and UV–vis was confirmed through similarity of the Raman spectra recorded at the beginning (Fig. 8(a)) and at the end (Fig. 8(c)) of the first cycle in a experiment recorded in the potential range from −0.20 to 0.80 V.

Analyzing the above data together with the cyclic voltammetry and 'in situ' UV–vis measurements, we have concluded that during the first cycle, the oxidation of PPSA starts by the N atom and its respective polarons (I) are the only oxidized species present (Scheme 2). This redox process is reversible. When the oxidation proceeds, bipolarons (II) are formed due to oxidation of the sulfur atom. During the reduction, the bipolarons (II) are converted to polarons (III) (Scheme 2).

A plausible explanation to understand why the N atom loses its lone electron easier than the sulfur is based on the molecule geometry. The X-rays data [11] of a molecule composed of two monomeric units of the PPSA, shows that the lone electron pair of the nitrogen is in an orbital at almost perpendicular position in relation to the aromatic ring orbital, being more available to be removed. This fact is not observed with the respective orbital of the sulfur atom, which presents some delocalization with the aromatic ring. This preference for the heteroatoms can also be explained, taking into account that if the heteroatoms lose electrons, its original hybridization sp^3 acquires a certain sp^2 character, which increases the coplanarity and consequently the delocalization of the electrons.

Analyzing the Raman spectra obtained during the second scan (Fig. 9), it was observed that those recorded during the oxidation at 1.20 V (Fig. 9(b)) and at 2.00 V (Fig. 9(c)) have

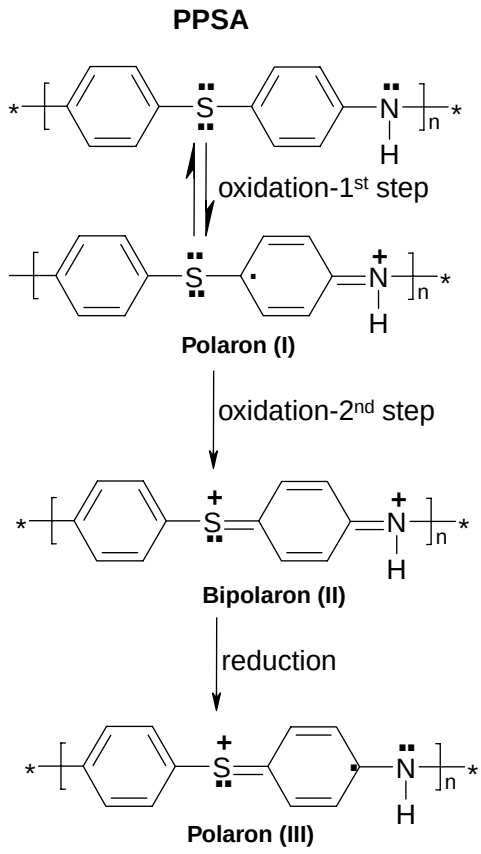

Scheme 2. Complete mechanism for the redox process of the PPSA during the first scan.

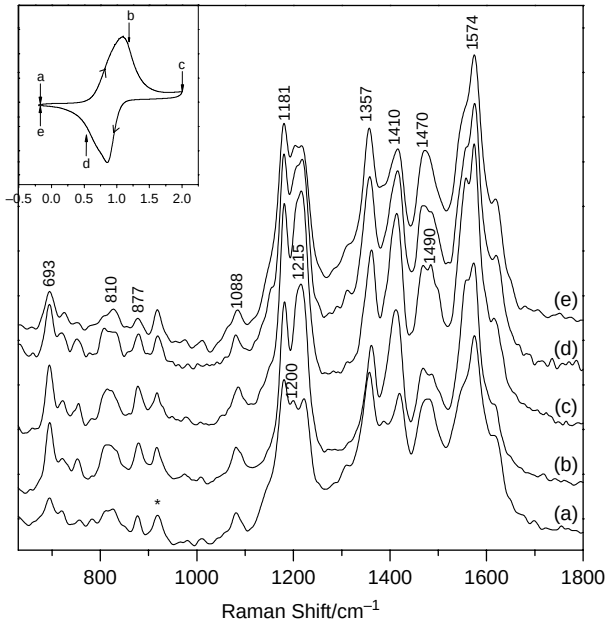

Fig. 9. Raman spectra of a PPSA film recorded during the second scan in the potential range: −0.2–2.0 V (a) −0.20 V (b) 1.20 V (c) 2.00 (d) 0.50 V (e) −0.20 V.

shown a slight increase of the bands related to the presence of quinoid units (693, 810, 877 and 1410 cm^{-1}). In addition, it was verified that the bands at 1215 and 1490 cm^{-1} suffer alterations as the oxidation proceeds. Since these bands are related to the carbon–nitrogen bond, we can infer that the formation of bipolarons is due to the oxidation of the nitrogen site. The band at 1088 cm^{-1} remains unaffected, suggesting that the C–S single bond character has not changed. During the reduction, the changes display an inverse behavior to that mentioned during the oxidation (Fig. 9(d) and (e)). These results indicate that the transformation of bipolarons to polarons occurs due to the reduction of the nitrogen. The similarity between the spectra recorded at the beginning (Fig. 9—spectrum a) and at the end (Fig. 10—spectrum e) of the second scan confirms the reversibility of this cycle. The subsequent cycles have shown the same behavior. Based on these data and the CV and 'in situ' UV–vis, we have concluded that in the second and subsequent cycles polarons (III) are oxidized to bipolarons (II) and vice versa (Scheme 3), mainly by oxidation of the N atom.

3.5. 'In situ' resistance measurements

In order to investigate the resistance changes that the copolymer suffers during the electrochemical doping, 'in situ' resistance experiments of a PPSA film deposited on Au electrode, using 0.2 M of $LiClO_4$ in propylene carbonate as the electrolytic solution, were carried out. The graphs in Fig. 10 are in logarithm scale, plotting the resistance of the film (R_f) as a function of the applied potential (E) recorded during the first and second scan.

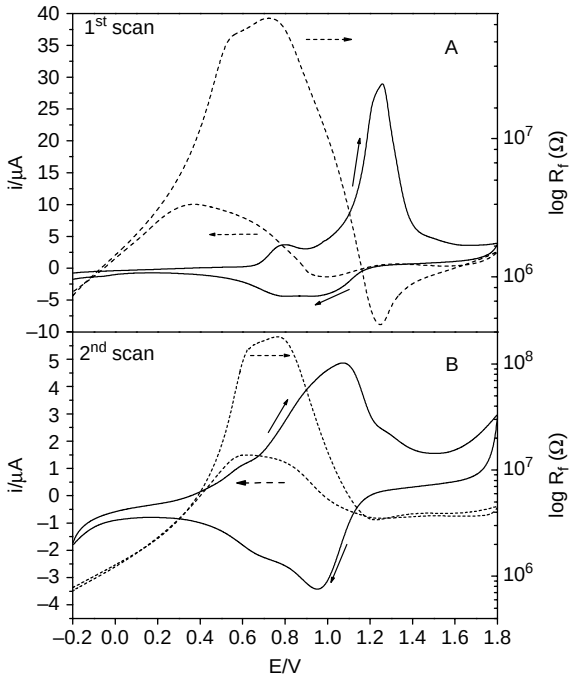

Fig. 10. Graphs of log R_f versus E of PPSA film deposited on Au electrode in 0.2 M $LiClO_4$/PC ($v = 0.001$ V s^{-1}) (—) Current (– – –) log R_f.

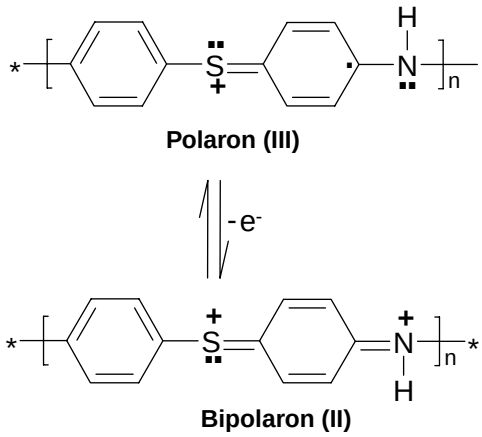

Scheme 3. Complete mechanism for the redox process of PPSA during the second and subsequent cycles.

During the oxidation of the PPSA in the first scan (Fig. 10(A)), it was observed that the resistance of the film increases markedly up to 0.50 V. This behavior was attributed to the increase of the contact resistance of the film-solution produced by the polarization of the electrode. Between 0.50 and 0.75 V the resistance of the material increases less strongly in spite of the appearance of the first anodic wave. Between 0.75 and 1.25 V the resistance of the film decreases markedly, coinciding with the second anodic wave. During the reduction process, the increase in the resistance occurs when the cathodic wave appears.

During the second cycle (Fig. 10(B)), the decrease of the resistance of the film starts from 0.80 V and coincides with the increase of the anodic current. After 1.25 V, the value of R_f remains constant, increasing again when the cathodic process emerges. All the subsequent cycles present similar features.

Considering that during the first scan, the oxidation of the PPSA gives polarons and biporalons in the first and second anodic waves, respectively; we can infer that bipolaronic structures are the main conductive species for the reduction of film resistance. This conclusion is corroborated by two further observations: (a) the increase of the resistance during the reduction in the first scan, where bipolarons are converted to polarons and (b) in the subsequent cycle, the change of the resistance coincides with the same species (bipolarons) were also suggested as free charge carries by Temperini et al. in the doped poly(diphenylamine) (PDPA), a polymer similar to PANI. In the case of PANI, polarons are responsible for the high conductivity [32].

4. Conclusions

In this work we have investigated the electrochemical behavior of a new copolymer of poly(aniline) and poly(phenylene sulfide) in organic media by cyclic voltammetry associated with spectroscopic techniques (UV–vis and Raman). We have shown that during the oxidation in the first voltammetric scan, the N atom is the first site to be oxidized, generating polarons. Further oxidation has led to the formation of bipolarons by oxidation of the sulfur atom. The latter process

is irreversible and the reduction of these bipolarons resulted in polarons with different structure than the ones formed in the first stage. In the second and subsequent scans, the redox process becomes more reversible and polarons are oxidized to bipolarons and vice-versa. The 'in situ' resistance measurements have proved that bipolarons are the free charge carriers in the doped PPSA, distinctly that it is observed with PANI.

Acknowledgements

This work was supported by FAPESP (Procs: 03/07568-0 and 03/10015-3) and CNPq (CT-Energ 400562/2003-0). Fellowships from FAPESP (F. F. C. Bazito-Proc: 97/12943-2) and CNPq (S.I.C. de Torresi) are gratefully acknowledged. Authors are also indebted to Professors Y. Kawano and R. Torresi for the TG/DSC and 'in situ' resistance measurements and to Laboratory of spectroscopy molecular (LEM) for the Raman facilities.

Supplementary data

Supplementary data associated with this article can be found at doi:10.1016/j.polymer.2005.11.076

References

[1] Genies EM, Noel P. J Electroanal Chem 1991;310(1–2):89–111.
[2] Li S, Dong H, Cao Y. Synth Met 1989;29(1):329–36.
[3] Bae WJ, Jo WH, Park YH. Synth Met 2003;132(3):239–44.
[4] Dao LH, Leclerc M, Guay J, Chevalier JW. Synth Met 1989;29(1):377–82.
[5] Park JW, Shin HC, Lee Y, Son Y, Baik DH. Macromolecules 1999;32(14):4615–8.
[6] Winokur MJ. In: Skothein TA, Elsenbaumer RL, Reynolds JR, editors. Handbook of conducting polymers. New York: Marcel Dekker; 1997. p. 708–25.
[7] Brady DG. J Appl Polym Sci 1981;20(9):2541–51.
[8] Freund L, Heitz W. Makromol Chem 1990;191:815–28.
[9] Magno F, Bontempelli G, Pillon G. J Electroanal Chem 1971;30(3):375–83.
[10] Wang LX, Guth TS, Havinga E, Mullen K. Angew Chem Int Ed 1996;35(13–14):1495–7.
[11] Leuninger J, Wang C, Guth TS, Enkelmann V, Pakula T, Mullen K. Macromolecules 1998;31(6):1720–7.
[12] Li GF, Josowicz M, Janata J, Mullen K. J Phys Chem B 2001;105(11):2191–6.
[13] Bassler H, Tak YH, Leuninger J, Mullen K. J Phys Chem B 1998;102(25):4887–91.
[14] Hiemenz PC, Rajagopalan R. Principles of colloid and surface chemistry. 3rd ed. New York: Marcel Dekker; 1997.
[15] Csahok E, Vieil E, Inzelt G. J Electroanal Chem 2000;482(2):168–77.
[16] Leuninger J, Uebe J, Salbeck J, Gherghel L, Wang C, Mullen K. Synth Met 1999;100(1):79–88.
[17] Genies EM, Syed A, Tsintavis C. Mol Cryst Liq Cryst 1985;121(1–4):181–6.
[18] Ikkala OT, Pietilä L-O, Ahjopalo L, Österholm H, Passiniemi PJ. J Chem Phys 1995;103(22):9855–63.
[19] Quillard S, Berrada K, Louarn G, Lefrant S. New J Chem 1995;19(4):365–74.
[20] Pekmez N, Pekmez K, Yildiz A. J Electroanal Chem 1994;370(1–2):223–9.
[21] Lapkowski M, Berrada K, Quillard S, Louarn G, Lefrant S, Pron A. Macromolecules 1995;28(4):1233–8.
[22] Watanabe A, Mori K, Mikuni M, Nakamura Y, Matsuda M. Macromolecules 1989;22(8):3323–7.
[23] Huang WS, MacDiarmid AG. Polymer 1993;34(9):1833–45.
[24] Stilwell DE, Park SM. J Electrochem Soc 1989;136(2):427–33.
[25] Bredas JL, Street GB. Acc Chem Res 1985;18(10):309–15.
[26] Arsov LD, Plieth W, Kossmehl G. J Solid State Chem 1998;2(5):355–61.
[27] Silva JEP, Faria DLA, Torresi SIC, Temperini MLA. Macromolecules 2000;33(8):3077–83.
[28] Silva JEP, Torresi SIC, Faria DLA, Temperini MLA. Synth Met 1999;101(1–3):834–5.
[29] Silva JEP, Temperini MLA, Torresi SIC. Electrochim Acta 1999;44(12):1887–91.
[30] Piaggio P, Musso GF, Dellepiane G. J Phys Chem 1995;99(12):4187–92.
[31] Sathyanarayana DN, Raja KVS. Spectrochim Acta Part A 1985;41(6):809–13.
[32] do Nascimento GM, Torresi SIC, Temperini MLA, Silva JEP. Macromolecules 2002;35(1):121–5.